

# RSC Advances



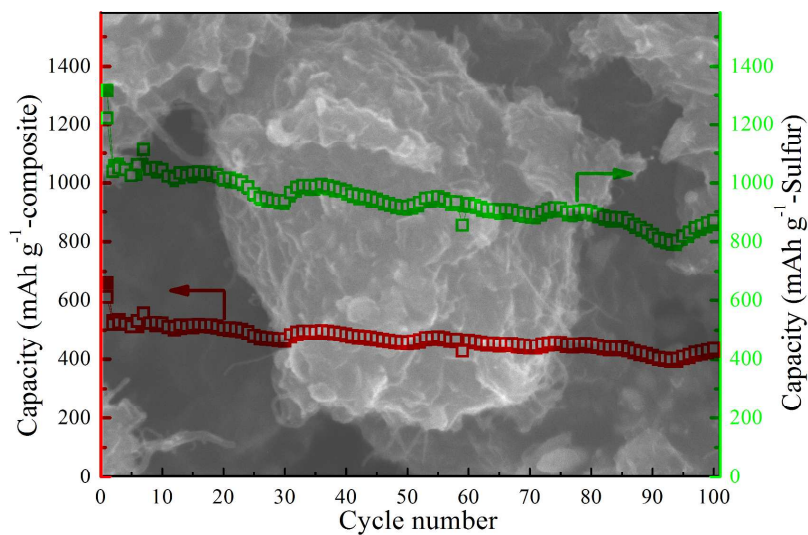
This is an *Accepted Manuscript*, which has been through the Royal Society of Chemistry peer review process and has been accepted for publication.

*Accepted Manuscripts* are published online shortly after acceptance, before technical editing, formatting and proof reading. Using this free service, authors can make their results available to the community, in citable form, before we publish the edited article. This *Accepted Manuscript* will be replaced by the edited, formatted and paginated article as soon as this is available.

You can find more information about *Accepted Manuscripts* in the [Information for Authors](#).

Please note that technical editing may introduce minor changes to the text and/or graphics, which may alter content. The journal's standard [Terms & Conditions](#) and the [Ethical guidelines](#) still apply. In no event shall the Royal Society of Chemistry be held responsible for any errors or omissions in this *Accepted Manuscript* or any consequences arising from the use of any information it contains.

## Graphical Abstracts



Graphene wrapped sulfur/carbon nanotubes composite is prepared via the designing ball-milling route, which can help realize large-scale synthesis of electrode materials with good consistency. The obtained composite shows high discharge capacity and good cycle performance.

Cite this: DOI: 10.1039/c0xx00000x

www.rsc.org/xxxxxx

## ARTICLE TYPE

# Graphene wrapped sulfur-based composite cathodes: ball-milling synthesis and high discharge capacity

Zhong Su<sup>a</sup>, Chenglong Gao<sup>b</sup>, Hanlin Li<sup>a</sup>, Sanjay Nanda<sup>b</sup>, Chao Lai<sup>a,b</sup>, Kai Xi<sup>b</sup>

Received (in XXX, XXX) Xth XXXXXXXXX 20XX, Accepted Xth XXXXXXXXX 20XX

DOI: 10.1039/b000000x

A facile ball-milling route, which can help realize large-scale synthesis, is developed to prepare graphene wrapped sulfur/carbon nanotubes composite. Electrochemical tests show that the obtained composite demonstrates high sulfur utilization and good cycle performance. Calculated by the total mass of the composite, a high reversible capacity of 626.0 mAh g<sup>-1</sup> can be obtained after 70<sup>th</sup> cycle at the current density of 400 mA g<sup>-1</sup>.

## Introduction

The urgent demand for high-power and high-energy-density battery systems has spurred extensive research in developing novel electrode materials, in response to the development of electric vehicles (EVs) and hybrid electric vehicles (HEVs). Elemental sulfur has been proposed as one of the most promising cathode materials for next-generation high-energy density rechargeable batteries due to its high theoretical capacity of 1672 mAhg<sup>-1</sup>, as well as environmental friendliness, abundance, and economic price.<sup>1-3</sup> Despite these advantages, the commercialization of Li-S batteries are still seriously limited by the low sulfur utilization and poor cycle life, arising from the insulating nature of sulfur ( $5 \times 10^{-30} \Omega^{-1} \text{cm}^{-1}$  at 25 °C) and dissolution of polysulfides. During the discharge/charge process, the generated higher-order polysulfides can diffuse through the electrolyte to anode and react with the lithium anode to form lower-order polysulfides. These reduced products can also diffuse back to the sulfur cathode, and this cyclic process is known as the “shuttle effect”.<sup>1-3</sup> Such a parasitic process results in poor cycle life, low coulombic efficiency and low utilization of sulfur active material. To address these problems, there have been extensive investigations into improving sulfur cathodes by using conductive carbon as the sulfur immobilizer and conductive matrix.<sup>1-3</sup> Among those carbon materials, graphene are of particular interest due to its large surface area (ca. 2600 m<sup>2</sup> g<sup>-1</sup>), excellent mobility of charge carriers (20000 cm<sup>2</sup> V<sup>-1</sup> s<sup>-1</sup>), high chemical and thermal stability, and superior mechanical flexibility.<sup>1-9</sup> For the composite based on the graphene and sulfur, significantly enhanced electrochemical performance has been obtained. However, due to the strong  $\pi$ - $\pi$  stacking and hydrophobic interactions, graphene sheets are easy to agglomerate during the experiment process, and always a complicated solution process is needed to obtain uniform graphene-based composites.<sup>4-9</sup> This will result in high

cost, and the consistency of the active material is also hardly controlled, seriously limiting their practical applications. Developing facile and large-scale synthetic routes to prepare homogeneous cathodes based on sulfur and graphene will assume immense importance to realize commercial lithium-sulfur batteries in subsequent research.

Ball-mill technology is widely used for grinding materials in industrial applications. For its application in the synthesis of electrode materials, the advantages can be described as follow: (1) large scale synthesis of homogeneous electrode materials can be easily realized, which is important for materials consistency of batteries; (2) reliable operation can ensure reproducible results; (3) it is suitable for various synthesis systems and appealing for practical application, due to its economy and easy replicability.<sup>10-13</sup> Following all the discuss above, we design a continuous ball-milling strategy to prepare a high performance graphene wrapped sulfur/carbon nanotubes composite. Firstly, sulfur and carbon nanotubes are homogeneously mixed via ball-milling. It has been suggested that sulfur particles will be closely attached to the surface of carbon nanotubes during ball-milling process, producing a highly uniform mixture.<sup>12-15</sup> Then, graphene oxide and hydrazine are added to produce a surface coating layer during the continuous ball-milling process. The hollow and cross-linked carbon nanotubes can ensure the fast transport of electrons from carbon to sulfur and facilitate lithium-ion diffusion throughout the whole material. The surface coating layer can further restrict the dissolution of polysulfide. The unique structure of the designed surface graphene-coating sulfur/carbon nanotubes composite can offer a high electrochemical performance.

## Experimental

### 2.1. Preparation and characterization

To prepare the precursor sulfur/carbon nanotubes composite (S/CNT composite), sulfur and multi-walled carbon nanotubes (diameter: 10-20nm, length: 5-15 $\mu$ m,  $\geq 95\%$ ) with a weight ratio of 3:2 were added in the agate tank (50 mL) and then mixed well by ball-milling. The ball-milling was performed in a planetary ball mill (QM-3SP04, Nanjing) under ambient conditions at a speed of 300 rpm for 3h. For the synthesis of graphene wrapped sulfur/CNT composite (graphene@S/CNT composite), graphene oxide (0.2 g, Tianjin Plannano Technology Co., Ltd) and S/CNT composite (0.4 g) were first distributed homogeneously in ethanol

(10 mL) by stirring. Then the mixture and hydrazine (1 mL, 35 wt% solution in water, Sigma Aldrich) were added in the agate tank and ball-milled at a speed of 500 rpm for 3h. The obtained sample was washed with water and ethanol, and dried at 60 °C for 12h.

The as-prepared samples were characterized by X-ray diffraction (XRD, Model LabX-6000, Shimadzu, Japan), Thermal Gravimetric Analysis (TGA, SDT Q600), scanning electron microscopy (SEM, JSM-7001F), and transmission electron microscopy (TEM, FEI Tecnai F20).

## 2.2 Electrochemical measurements

The working electrodes were prepared by compressing a mixture of active materials, acetylene black, and binder (polytetrafluoroethylene, PTFE) in a weight ratio of 70:20:10. Lithium metal was used as the counter and reference electrode. The electrolyte was Lithium bis(trifluoromethanesulfonyl)imide (2.8 M) dissolved in a mixture of dimethoxyethane (DME) and dioxolane (DOL) in a volume ratio of 1:1. The LAND-CT2001A galvanostatic testers were employed to measure the electrochemical capacity at a current density of 400 and 800 mA g<sup>-1</sup> and the cycle life of working electrodes at room temperature. The cut-off potentials for charge and discharge were set at 3.0 and 1.5 V (vs. Li<sup>+</sup>/Li), respectively. Cyclic voltammetry (CV) experiments were conducted using a CHI 600E potentiostat at a scan rate of 0.1 mV s<sup>-1</sup>.

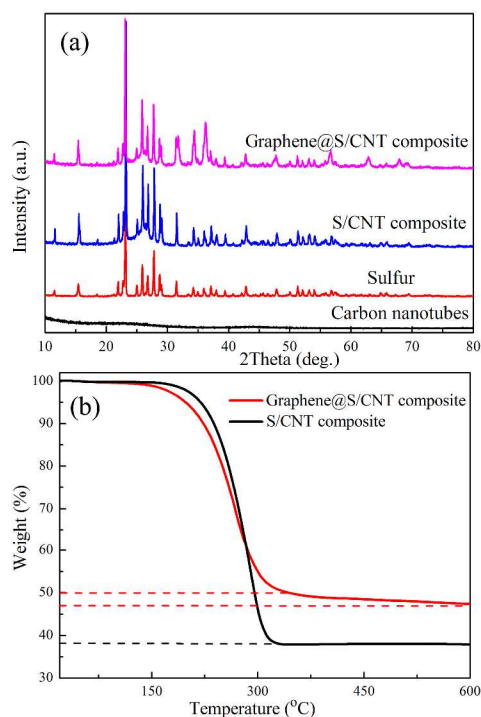


**Fig.1** XRD patterns of sulfur, carbon nanotubes, S/CNT composite and graphene@S/CNT composite (a); TGA Curves of the S/CNT composite and graphene@S/CNT composite (b).

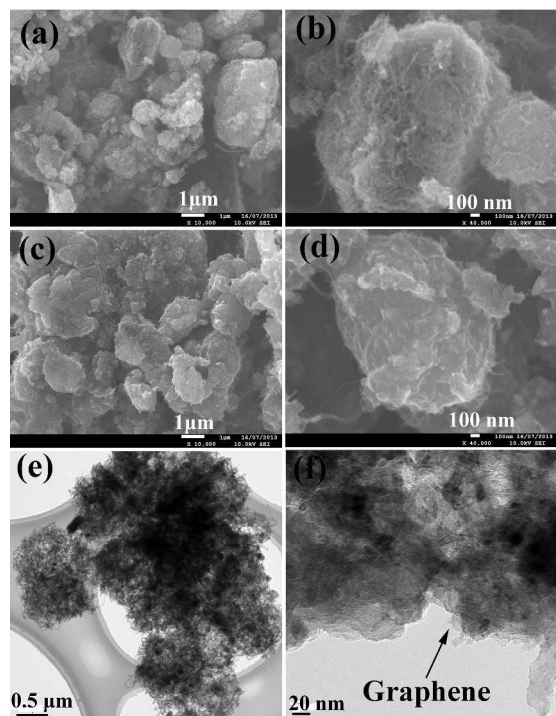
## 30 Results and discussion

Figure 1a includes the XRD patterns of sulfur, carbon nanotubes, S/CNT composite and graphene@S/CNT composite. As shown, different from previous thermal treatment routes,<sup>16,17</sup> the

crystalline state of sulfur is well retained after ball-milling. The graphene@S/CNT composite demonstrates a similar pattern as S/CNT composite due to the amorphous state of graphene, and also weaker peaks of the sulfur due to the coating of graphene. Fig. 1b is the TGA curves of the S/CNT composite and graphene@S/CNT composite obtained at a heating rate of 10 °C min<sup>-1</sup> under the protection of Argon. As shown, the sulfur content in the graphene@S/CNT composite is ca. 50 wt%. Furthermore, it should be mentioned that there are extra 4 wt% loss till 600 °C for the graphene wrapped composite, while the curves of S/CNT is flat. The extra weight loss may also be attributed to the evaporation of sulfur, as the violent ball-milling process will generate a tight coating layer, and even produce a weak binding between graphene and sulfur. Similar to sulfur/nanoporous carbon composite, a higher temperature is needed to conquer the restriction of such coating or binding.<sup>18</sup>

SEM was carried out to illustrate the morphology of the as-prepared samples. As shown in Figure 2a and 2b, it is obvious that the S/CNT composite is micro-sized particles with cross-linked carbon nanotubes. There are no sulfur particles that can be observed, indicating the homogenous mixture of sulfur and carbon nanotubes. For the graphene@S/CNT composite, different morphology is observed. It can be seen that there is further aggregation of the composite particles, coated by graphene. The reduction of graphene oxides leads to shrinkage and re-stacking of graphene nanosheets,<sup>19</sup> thus wrapping the particles together to form the surface-coated composite. Comparing Figure 2b and 2d, it can be seen that the loose cross-linked structure disappears, and the S/CNT composite is completely encapsulated by the graphene coating layer. To further illustrate the microstructure of the sulfur-based composite, TEM images are shown in Figure 2e and 2f. For the graphene@S/CNT composite, it is obvious that the reduced graphene sheets encapsulate the S/CNT composite particles to form a hierarchical structure, and the surface coating graphene layer can be clearly observed in Figure 2f. It should be mentioned that small amounts of nanotubes are not well wrapped, and further research focused on the ball-milling speed or solvent is still needed to obtain more uniform composite. On the other hand, the exposed nanotubes also can facilitate the transport of electrolyte ions into the composite to produce a high electrochemical performance.

Figure 3 is the cyclic voltammograms (CVs) of as-prepared S/CNT composite and graphene@S/CNT composite at the scan rate of 0.1 mV s<sup>-1</sup>. Two obvious different curves can be observed. For the graphene coating composite, during the initial cathodic process, a pair of peaks around 2.18 and 1.85 V can be observed, and which involves the two-step reduction of S<sub>8</sub> to lithium polysulfides and eventually to Li<sub>2</sub>S.<sup>1-3</sup> Different from previous reports,<sup>6-8,16,17,20,21</sup> the second peak is obviously broadened. The possible reason can be attributed to the tight package of graphene during the ball-milling process and strong adsorption ability of carbon nanotubes, thus leading to high electrochemical polarization.<sup>22</sup> For the S/CNT composite, only one cathodic peak around 2.1 V can be observed due to the dissolution of Li<sub>2</sub>S<sub>8</sub>, further confirming the restriction effect of graphene in the graphene@S/CNT composite.

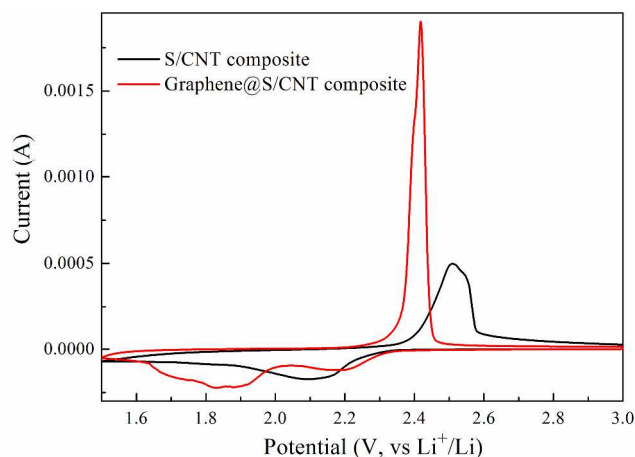


**Fig.2** SEM and TEM images of S/CNT composite (a,b) and graphene@S/CNT composite(c,d,e,f).

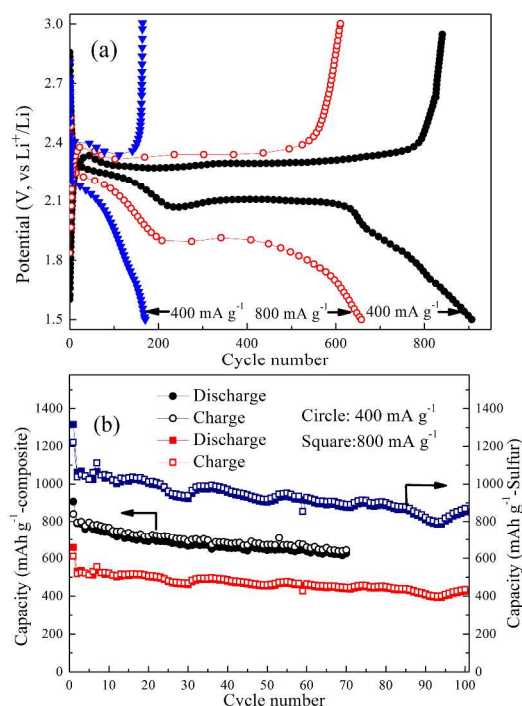
Based on the above results, it can be concluded that the obtained composite contains a cross-linked conductive matrix, hollow channels and tight surface coating graphene layer, which make it a promising high-performance sulfur-based cathode. To evaluate the electrochemical performance of the as-prepared samples, cell tests are conducted (Figure 4). Figure 4a includes the initial discharge-charge curves of obtained composites at the current density of 400 and 800 mA g<sup>-1</sup>. For the S/CNT composite, it demonstrates a low discharge and charge capacity of 170 and 164 mAh g<sup>-1</sup> at the current density of 400 mA g<sup>-1</sup>, respectively. In comparison, the graphene@S/CNT composite presents a different discharge-charge curve, and a flat potential plateau around 2.1V can be observed, which corresponds to the transfer from S<sub>8</sub><sup>2-</sup> to lower-order polysulfide.<sup>1-3</sup> Without graphene wrapping, the S<sub>8</sub><sup>2-</sup> ions will dissolve into the electrolyte before the transformation, and the conventional flat plateau disappear, accounting for sulfur/carbon nanotubes composite, in consistent with the result of CVs. On the other hand, the initial discharge and charge capacity of graphene@S/CNT composite is 906.6 and 840.3 mAh g<sup>-1</sup>, while it is about 1813.2 and 1680.6 mAh g<sup>-1</sup> calculated by weight of sulfur, further confirming the restriction on the dissolution of polysulfides introduced by the graphene coating. The high initial discharge capacity exceeding the theoretical capacity of sulfur also can be observed in other sulfur/carbon composite.<sup>18,23,24</sup> However, if the extra weight loss (4 wt%) of the graphene wrapped composite is attributed to the loss of sulfur, the initial discharge capacity calculated by the sulfur is 1678 mAh g<sup>-1</sup>, perfectly equal to the theoretical capacity of element sulfur. When the current density is enhanced to 800 mA g<sup>-1</sup>, it is obvious that the discharge-charge curves are well-retained, and the initial discharge capacity is 658 mAh g<sup>-1</sup>. The capacity retention can reach to 72.6%, indicating the good kinetic process of the composite.

Figure 4b includes the cycle curves of obtained composites at different current densities. As shown, the graphene@S/CNT composite shows good cycle performance, and after 70 cycles, the discharge capacity can be retained at 626.0 mAh g<sup>-1</sup> at the current density of 400 mA g<sup>-1</sup>, which is about 1252.0 mAh g<sup>-1</sup> calculated by the sulfur. Furthermore, it is worth mentioning that the composite shows a high coulombic efficiency above 95% after 2<sup>nd</sup> cycle. The reversible discharge capacity (1256.0 mAh g<sup>-1</sup>) is among the best results compared to the graphene and sulfur based composites synthesized by other methods,<sup>7-9,25-29</sup> indicating that the ball-milling route is the practical route for large-scale synthesis of high performance sulfur-based composite. At the current density of 800 mA g<sup>-1</sup>, it can be seen that the obtained composite still shows a good cycle performance and after 100<sup>th</sup> cycle, a discharge capacity of 425.8 mAh g<sup>-1</sup> is obtained which is about 851.6 mAh g<sup>-1</sup> calculated by weight of sulfur. It should be emphasized that although the sulfur content is low, the graphene@S/CNT composite still demonstrates a high discharge capacity calculated by the composite due to high sulfur utilization. The high reversible capacity of 626.0 mAh g<sup>-1</sup> among the best results even compared to the graphene and sulfur-based composite prepared via complicated solution synthesis process and/or template.<sup>4,5,7-9,25-27</sup>

By considering all the results above, it can be concluded that that high discharge capacity has been obtained by a simple ball-milling route, without employing complex solution synthesis or thermal treatment processes. The high performance of graphene@S/CNT composite can be attributed to its unique structure elaborated as follows: 1) the hollow carbon nanotubes conductive matrix can ensure fast electrons and Li-ions transport throughout the composite, thus producing a high sulfur utilization at high current density; 2) the intact hollow tubes of carbon nanotubes can trap the polysulfides and accommodate volume change to maintain structural stability of the composite during the discharge-charge process; 3) the homogeneous and tight surface coating of graphene can effectively restrict the dissolution of polysulfides and further enhance the utilization of sulfur due to its excellent conductivity. In conclusion, same high performance sulfur-based composites can be obtained via practical ball-milling route as compared to complicated solution route.



**Fig.3** Cyclic voltammograms of the S/CNT composite and graphene@S/CNT composite at scan rate of 0.1 mV s<sup>-1</sup>.



**Fig.4** Initial discharge/charge curves (a) and cycle performance (b) of the graphene@S/CNT composite and S/CNT composite at different current densities (composite); cycle performance (c) of the graphene@S/CNT composite at different current densities (composite).

## Conclusions

Graphene-wrapped sulfur/carbon nanotubes composite is successfully prepared via the ball milling method. Compared to previous solution-based methods, large-scale synthesis of graphene-wrapped sulfur composite with high consistency can be easily achieved by this strategy. Homogeneous coating of graphene on the sulfur/carbon nanotubes composite can be observed from the SEM and TEM characterization, leading to the high electrochemical performance of the obtained composite. At a current density of 400 mA g<sup>-1</sup>, the graphene@S/CNT composite demonstrates a high initial discharge capacity of 906.6 mAh g<sup>-1</sup> and a good cycle performance. After the 70<sup>th</sup> cycle, the capacity can be stabilized at 626.0 mAh g<sup>-1</sup> calculated by the total mass of composite. When the current density is increased to 800 mA g<sup>-1</sup>, the discharge capacity still reaches 658.0 mAh g<sup>-1</sup>, and the capacity is retained 426.8 mAh g<sup>-1</sup> after 100 cycles, which is 851.6 mAh g<sup>-1</sup> calculated by weight of sulfur. The good performance can be attributed to the synergistic effect of graphene coating, carbon conductive matrix and intact hollow tubes. The design continuous ball-milling route also can be applied to prepare other graphene wrapped sulfur-carbon materials.

## Acknowledgements

This work has been supported by the Chinese National Science Funds (No. 51202094); the Priority Academic Program Development of Jiangsu Higher Education Institutions; the Natural Science Foundation (No. 12KJB150010) of Jiangsu Education Committee of China.

## Notes and references

- <sup>a</sup>School of Chemistry and Chemical Engineering, and Jiangsu Key Laboratory of Green Synthetic Chemistry for Functional Materials, Jiangsu Normal University, Xuzhou, Jiangsu 221116, China, Email: laichao@jsnu.edu.cn;
- <sup>b</sup>Department of Materials Science and Metallurgy, University of Cambridge, Cambridge, CB2 3QZ, UK.
- 1 A. Manthiram, Y.Z. Fu and Y.S. Su, *Acc. Chem. Res.*, 2013, **46**, 1125..
  - 2 S. Evers and L.F. Nazar, *Acc. Chem. Res.*, 2013, **46**, 1135.
  - 3 D. Bresser, S. Passerini and B. Scrosati, *Chem. Commun.*, 2013, **49**, 10545.
  - 4 M. Xiao, M. Huang, S.S. Zeng, D.M. Han, S.J. Wang, L.Y. Sun and Y.Z. Meng, *RSC Advances*, 2013, **3**, 4914.
  - 5 G. He, C.J. Hart, X. Liang, A. Garsuch and L.F. Nazar, *ACS Appl. Mater. Interfaces*, 2014, **6**, 10917.
  - 6 N. Mahmood, C.Z. Zhang, H. Yin and Y.L. Hou, *J. Mater. Chem. A*, 2014, **2**, 15.
  - 7 J. Xie, J. Yang, X.Y. Zhou, Y.L. Zou, J.J. Tang, S.C. Wang and F. Chen, *J. Power Sources*, 2014, **253**, 55.
  - 8 R.J. Chen, T. Zhao, J. Lu, F. Wu, L. Li, J.Z. Chen, G.Q. Tan, Y.S. Ye and K. Amine, *Nano Lett.*, 2013, **13**, 4642.
  - 9 S.T. Lu, Y.W. Cheng, X.H. Wu and J. Liu, *Nano Lett.* 2013, **13**, 2485.
  - 10 C. Lai, Z.Z. Wu, Y.X. Zhu, Q.D. Wu, L. Li and C. Wang, *J. Power Sources*, 2013, **226**, 71.
  - 11 L.Z. Ouyang, L.N. Guo, W.H. Cai, J.S. Ye, R.Z. Hu, J.W. Liu, L.C. Yang and M. Zhu, *J. Mater. Chem. A*, 2014, **2**, 11280..
  - 12 X.-B. Cheng, J.-Q. Huang, Q. Zhang, H.-J. Peng, M.-Q. Zhao and F. Wei, *Nano Energy*, 2014, **4**, 65.
  - 13 L. Zhu, W.C. Zhu, X.-B. Cheng, J.-Q. Huang, H.-J. Peng, S.-H. Yang and Q. Zhang, *Carbon*, 2014, **75**, 161.
  - 14 J.Z. Chen, F. Wu, R.J. Chen, L. Li and S. Chen, *New Carbon Mater.*, 2013, **28**, 428.
  - 15 W. Weng, S.W. Yuan, N. Azimi, Z. Jiang, Y.Z. Liu, Y. Ren, A. Abouimrane and Z.C. Zhang, *RSC Adv.*, 2014, **4**, 27518.
  - 16 G.-C. Li, G.-R. Li, S.-H. Ye and X.-P. Gao, *Adv. Energy Mater.*, 2012, **2**, 1238.
  - 17 X.F. Wang, X.P. Fang, X.W. Guo, Z.X. Wang and L.Q. Chen, *Electrochim. Acta*, 2013, **97**, 238.
  - 18 J. Kim, D.-J. Lee, H.-G. Jung, Y.-K. Sun, J. Hassoun and B. Scrosati, *Adv. Funct. Mater.*, 2013, **23**, 1076.
  - 19 S.F. Pei and H.-M. Cheng, *Carbon*, 2012, **50**, 3210.
  - 20 N. Jayaprakash, J. Shen, S.S. Moganty, A. Corona and L.A. Archer, *Angew. Chem. Int. Ed.*, 2011, **123**, 1.
  - 21 Y.-S. Su and A. Manthiram, *Nat. Commun.*, 2012, **3**, 1166.
  - 22 J.L. Wang, J. Yang, J.Y. Xie, N.X. Xu and Y. Li., *Electrochem. Commun.*, 2002, **4**, 499.
  - 23 D.-J. Lee<sup>1</sup>, M. Agostini, J.-W. Park, Y.-K. Sun, J. Hassoun and B. Scrosati, *ChemSusChem*, 2013, **6**, 2245.
  - 24 S.S. Zhang, *Frontiers in Energy Research*, 2013, **1**, 1.
  - 25 H.-Jie Peng, J.-Q. Huang, M.-Q. Zhao, Q. Zhang, X.-B. Cheng, X.-Y. Liu, W.-Z. Qian and F. Wei, *Adv. Funct. Mater.*, 2014, **24**, 2772.
  - 26 W.Z. Bao, Z. Zhang, W. Chen, C.K. Zhou, Y.Q. Lai and J. Li, *Electrochim. Acta*, 2014, **127**, 342.
  - 27 B. Wang, Y.F. Wen, D.L. Ye, H. Yu, B. Sun, G.X. Wang, D. Hulicova-Jurcakova and L.Z. Wang, *Chem. Eur. J.*, 2014, **20**, 5224.

- 
- 28 K. H. Kim, Y.-Si Jun, J.A. Gerbec, K.A. See, G.D. Stucky, H.-T. Jung, *Carbon*, 2014, **69**, 543.
- 29 J.-Q. Huang, H.-J. Peng, X.-Y. Liu, J.-Q. Nie, X.-B. Cheng, Q. Zhang and F. Wei, *J. Mater. Chem. A*, 2014, **2**, 10869

5

10